International Telecommunication Union

ITU-R

Radiocommunication Sector of ITU

Recommendation ITU-R P.1407-8

(09/2021)

Multipath propagation and parameterization of its characteristics

P Series

Radiowave propagation

International Telecommunication Union

Foreword

The role of the Radiocommunication Sector is to ensure the rational, equitable, efficient and economical use of the radio-frequency spectrum by all radiocommunication services, including satellite services, and carry out studies without limit of frequency range on the basis of which Recommendations are adopted.

The regulatory and policy functions of the Radiocommunication Sector are performed by World and Regional Radiocommunication Conferences and Radiocommunication Assemblies supported by Study Groups.

Policy on Intellectual Property Right (IPR)

ITU-R policy on IPR is described in the Common Patent Policy for ITU-T/ITU-R/ISO/IEC referenced in Resolution ITU-R 1. Forms to be used for the submission of patent statements and licensing declarations by patent holders are available from http://www.itu.int/ITU-R/go/patents/en where the Guidelines for Implementation of the Common Patent Policy for ITU-T/ITU-R/ISO/IEC and the ITU-R patent information database can also be found.

Series of ITU-R Recommendations

(Also available online at http://www.itu.int/publ/R-REC/en)

Series	Title
BO	Satellite delivery
BR	Recording for production, archival and play-out; film for television
BS	Broadcasting service (sound)
BT	Broadcasting service (television)
F	Fixed service
M	Mobile, radiodetermination, amateur and related satellite services
P	**Radiowave propagation**
RA	Radio astronomy
RS	Remote sensing systems
S	Fixed-satellite service
SA	Space applications and meteorology
SF	Frequency sharing and coordination between fixed-satellite and fixed service systems
SM	Spectrum management
SNG	Satellite news gathering
TF	Time signals and frequency standards emissions
V	Vocabulary and related subjects

Note: *This ITU-R Recommendation was approved in English under the procedure detailed in Resolution ITU-R 1.*

Electronic Publication
Geneva, 2021

RECOMMENDATION ITU-R P.1407-8

Multipath propagation and parameterization of its characteristics

(Question ITU-R 203/3)

(1999-2003-2005-2007-2009-2013-2017-2019-2021)

Scope

Recommendation ITU-R P.1407 describes the nature of multipath propagation and defines the appropriate parameters for the statistical description of multipath effects, and provides examples of correlation effects among multiple propagation paths and their computation.

Keywords

Delay profiles, azimuth/elevation angle profiles, directional power-delay profile, Doppler, total power, multipath components

The ITU Radiocommunication Assembly,

considering

a) the necessity of estimating the effects of multipath on services employing digital systems;

b) that it is desirable to standardize the terminology and expressions used to characterize multipath,

recommends

1 that, to describe the concepts of multipath in a consistent manner, the terms and definitions given in Annex 1 should be employed;

2 that the correlation concepts of Annex 2 should be used to analyse the effects of multiple-input, multiple-output (MIMO) systems;

3 that for the generation of wideband channel, models in Annex 3 should be used to evaluate the performance of communication systems.

Annex 1

1 Introduction

In radio systems with low antenna heights, there are often multiple indirect paths between the transmitter and receiver due to reflections from surrounding objects, in addition to the direct path when there is line-of-sight. Such multipath propagation is particularly significant in urban environments, where the sides of buildings and paved road surfaces provide strong reflections. As a result, the received signal consists of the summation of several components having various amplitudes, phase angles and directions of arrival.

The resulting spatial variability of signal strength can be viewed as having two regimes:

a) rapid fading which varies over distances of the order of a wavelength due primarily to changes in phase angles of different signal components;

b) slow fading which varies over larger distances due primarily to changes in shadowing loss by surrounding objects.

In addition, the various signal components can be Doppler shifted by different amounts due to the movement of the mobile or of reflecting objects such as vehicles.

The multipath mobile channel can be characterized in terms of its impulse response which varies at a rate dependent on the speed of the mobile and/or the scatterers. Therefore, a receiver has to be able to cope with the signal distortion arising from echoes in the channel as well as the rapid changes in the nature of this distortion. Such characteristics of the mobile radio channel are described by the power delay profiles and the Doppler spectra which are obtained from wideband channel sounding measurements.

Signals transmitted to and from moving vehicles in urban or forested environments exhibit extreme variations in amplitude due to multiple scattering. Fades of 30 dB or more below the mean level are common. The instantaneous field strength when measured over distances of a few tens of wavelengths is approximately Rayleigh-distributed. The mean values of these small sector distributions vary widely from area to area, depending on the height, density and distribution of hills, trees, buildings and other structures.

Physically, multipath propagation parameters are multipath number, amplitude, path-length difference (delay), Doppler shift and arrival angle. These parameters can be characterized from a series of complex impulse responses over a short distance or time interval that can be used to estimate the delay-Doppler spread function representing the multipath phenomenon in the three dimensions of excess delay, Doppler frequency and power density. The delay-Doppler spread function defines a linear transversal filter whose output is the sum of multiple delayed, attenuated and Doppler-shifted replicas of the input signal. This formulation is useful for realizing a hardware simulator in the form of a dynamic transversal filter. The delay-Doppler spread function is used to estimate the power delay profile and the Doppler spectrum, which can be related to the coherence time of the channel. Alternatively, the Fourier transform of the time variant complex impulse response results in the time variant complex frequency response whose amplitude vs frequency characteristics define the multipath frequency selectivity, which is related to the correlation bandwidth and whose time variability gives the fading characteristics at a particular frequency.

Definitions of small-sector (or small-scale) channel parameters are given in §§ 2, 3 and 4. Statistics of small-scale parameters are subsequently used to produce cumulative distribution functions (CDFs). The medium-scale CDF covers a particular route of measurement, which is of the order of tens to hundreds of metres. The combined data set from a number of medium-scale routes is considered to be a large-scale or global characterization, which is representative of the surveyed environment, e.g. hilly terrain, urban, suburban, indoor large rooms, corridors, etc.

2 Parameters of delay profiles

2.1 Definitions of power delay profiles

The appropriate parameters for the statistical description of regarding multipath delay time can be computed from any of three types of power delay profiles: the instantaneous power delay profile; short-term power delay profile; or long-term power delay profile, which are either time averages obtained when the receiver is stationary and represent variations in the environment, or spatial averages obtained when the receiver is in motion.

Definitions of power delay profiles are given as shown in Fig. 1.

The instantaneous power delay profile is the power density of the impulse response at one moment at one point.

The short-term (small-scale) power delay profile is obtained by spatially averaging the instantaneous power delay profiles over several tens of wavelengths within the range where the same multipath components are maintained in order to suppress the variation of rapid fading. Alternatively, it can be obtained from the delay-Doppler spread function shown in Fig. 2A by taking the sum of the magnitude squared along the Doppler frequency shift axis, as illustrated in Fig. 2B.

FIGURE 1

Definition of power delay profiles

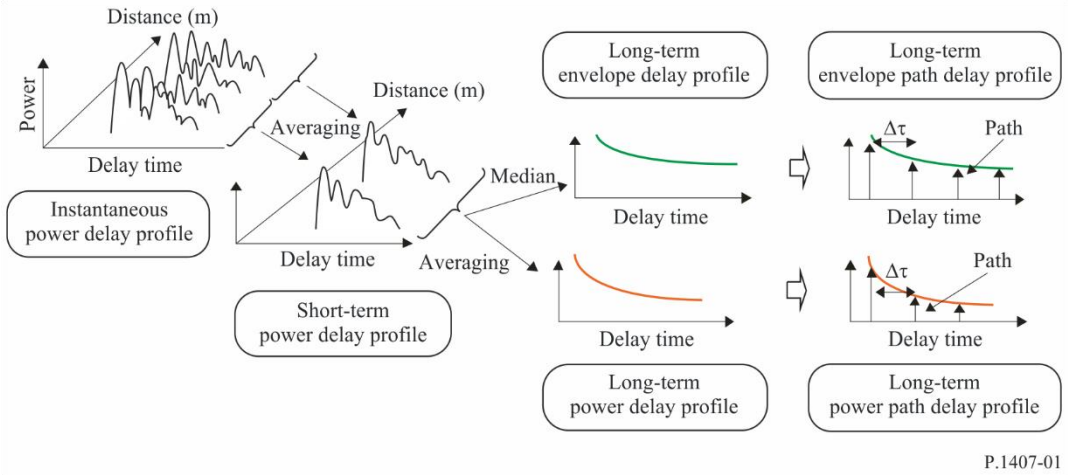

FIGURE 2A

Delay-Doppler spread function

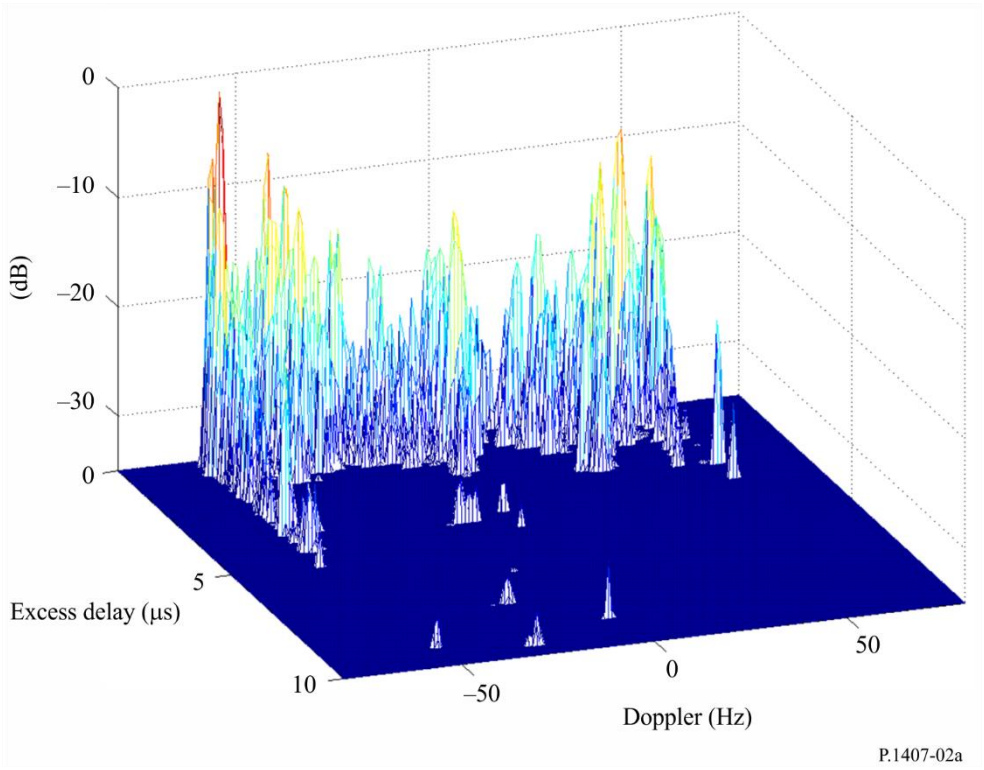

FIGURE 2B

Relative power versus time response

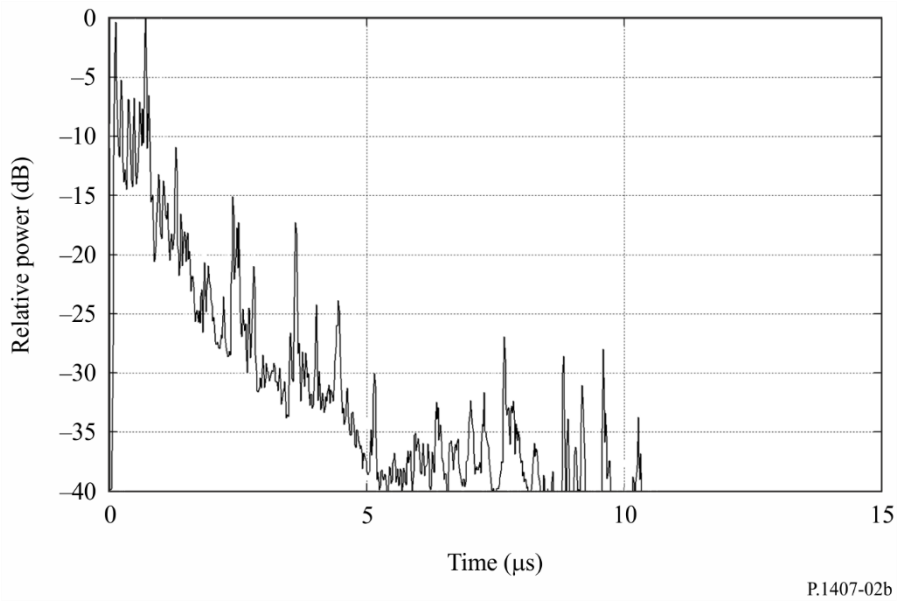

The long-term power delay profile is obtained by spatially averaging the short-term power delay profiles at approximately the same distance from the base station (BS) in order to suppress the variations due to shadowing.

Long-term power delay profiles with a discrete excess delay time normalized by time resolution 1/*B*, where *B* is the bandwidth, are defined as long-term power path delay profiles, instead of continuous power delay profiles.

On the other hand, the long-term envelope delay profile is the median value of the short-term power delay profiles at approximately the same distance from the base station; it expresses the shape of the delay profile at the area considered.

By taking the sum of the magnitude squared along the time delay axis of the delay-Doppler spread function the Doppler spectrum can be obtained as illustrated in Fig. 2C.

The short-term (small-scale) power delay profile is obtained by spatially averaging the instantaneous power delay profiles within the range where the same multipath components are maintained in order to suppress the variation of rapid fading as given in § 6. Alternatively, it can be obtained from the delay-Doppler spread function shown in Fig. 2A by taking the sum of the magnitude squared along the Doppler frequency shift axis, as illustrated in Fig. 2B.

FIGURE 2C

Doppler spectrum

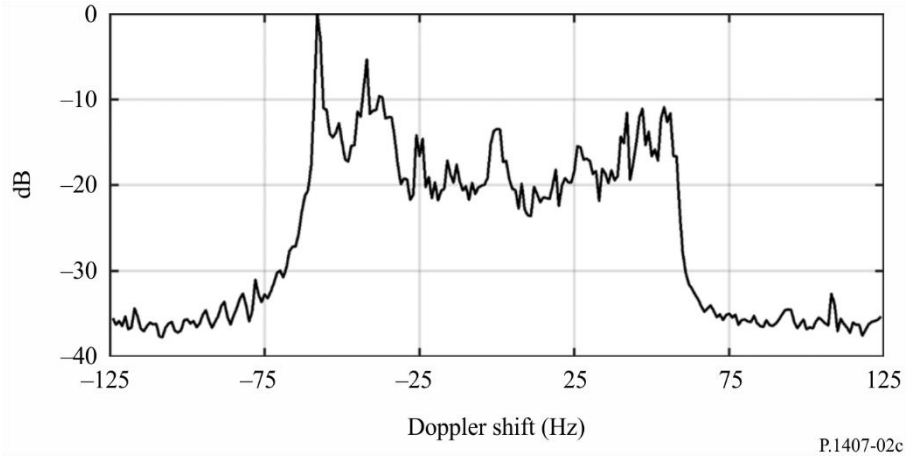

2.2 Definitions of statistical parameters

The appropriate parameters for the statistical description regarding multipath delay time are given below. The *average delay* is the power weighted-average of the excess delays measured and is given by the first moment of the power delay profile (the square of the amplitude of the impulse response).

The *r.m.s. delay spread* is the power weighted standard deviation of the excess delays and is given by the second moment of the power delay profile. It provides a measure of the variability of the mean delay.

The *delay window* is the length of the middle portion of the power delay profile containing a certain percentage (typically 90%) of the total power found in that impulse response.

The *delay interval* is defined as the length of the impulse response between two values of excess delay which mark the first time the amplitude of the impulse response exceeds a given threshold, and the last time it falls below it.

The *number of multipath or signal components* is the number of peaks in a power delay profile whose amplitude are within A dB of the highest peak and above the noise floor.

Definitions of the statistical parameters are given with reference to Figs 3A and 3B. It should be noted that the power delay profiles in the figures are represented in the decibel scale, however, the power summation equations are in linear units of power.

2.2.1 Total power

The *total power*, p_m, of the impulse response is:

$$p_m = \int_{t_0}^{t_3} p(t)\ \mathrm{d}\ t \tag{1}$$

where:

$p(t)$: power density of the impulse response in linear units of power

t: delay with respect to a time reference

t_0: instant when $p(t)$ exceeds the cut-off level for the first time

t_3: instant when $p(t)$ exceeds the cut-off level for the last time.

2.2.2 Average delay time

The average delay, T_D, is given by the first moment of the power delay profile:

$$T_D = \frac{\int_0^{\tau_e} \tau p(\tau)\ \mathrm{d}\tau}{\int_0^{\tau_e} p(\tau)\ \mathrm{d}\tau} - \tau_a \tag{2a}$$

where:

τ: excess time delay variable and is equal to $t - t_0$

τ_a: arrival time of the first received multipath component (first peak in the profile)

$\tau_e = t_3 - t_0$.

In discrete form with time resolution $\Delta\tau$ (= 1/B), equation (2a) becomes:

$$T_D = \frac{\sum_{i=1}^{N} \tau_i p(\tau_i)}{\sum_{i=1}^{N} p(\tau_i)} - \tau_M \tag{2b}$$

$$\tau_i = (i - 1)\ \Delta\tau = (i - 1)/B \qquad (i = 1, 2, \ldots..., N)$$

where $i = 1$ and N are the indices of the first and the last samples of the delay profile above the threshold level, respectively, and M is the index of the first received multipath component (first peak in the profile).

The delays may be determined from the following relationship:

$$t_i(\mu\mathrm{s}) = 3.3 r_i \qquad \mathrm{km} \tag{3}$$

where r_i is the sum of the distances from the transmitter to the multipath reflector, and from the reflector to the receiver, or is the total distance from the transmitter to receiver for t_{LoS}.

2.2.3 r.m.s. delay spread

The root mean square (r.m.s.) delay spread, S, is defined by the square root of the second central moment:

$$S = \sqrt{\frac{\int_0^{\tau_e} (\tau - T_D - \tau_a)^2\, p(\tau)\, \mathrm{d}\tau}{\int_0^{\tau_e} p(\tau)\, \mathrm{d}\tau}} \tag{4a}$$

In discrete form with time resolution $\Delta\tau$, equation (4a) becomes:

$$S = \sqrt{\frac{\sum_{i=1}^{N} (\tau_i - T_D - \tau_M)^2\, p(\tau_i)}{\sum_{i=1}^{N} p(\tau_i)}} \tag{4b}$$

2.2.4 Delay window

The delay window, W_q, is the length of the middle portion of the power delay profile containing a certain percentage, q, of the total power:

$$W_q = (t_2 - t_1) \tag{5}$$

whereby the boundaries t_1 and t_2 are defined by:

$$\int_{t_1}^{t_2} p(t)\,\mathrm{d}t = \frac{q}{100} \int_{t_0}^{t_3} p(t)\,\mathrm{d}t = \frac{q}{100}\, p_m \tag{6}$$

and the power outside of the window is split into two equal parts $\left(\frac{100 - q}{200}\right) p_m$.

2.2.5 Delay interval

The delay interval, I_{th}, is defined as the time difference between the instant t_4 when the amplitude of the power delay profile first exceeds a given threshold P_{th}, and the instant t_5 when it falls below that threshold for the last time:

$$I_{th} = (t_5 - t_4) \tag{7}$$

2.2.6 Number of multipath components

The number of multipath or signal components can be represented from the delay profile as the number of peaks whose amplitudes are within A dB of the highest peak and above the noise floor, as shown in Fig. 3B.

2.2.7 Recommended parameters

Delay windows for 50%, 75% and 90% power, delay intervals for thresholds of 9, 12 and 15 dB below the peak are recommended when analysing data. It is worth noting that the effects of noise and spurious signals in the system (from RF to data processing) can be very significant. Therefore, it is important to determine the noise and/or spurious threshold of the systems accurately and to allow a safety margin on top of that. A safety margin of 3 dB is recommended, and in order to ensure the integrity of results, it is recommended that a minimum peak-to-spurious ratio of, for example, 15 dB (excluding the 3 dB safety margin) is used as an acceptance criterion before an impulse response is included in the statistics. The threshold used for the identification of the number of multipath components depends on the dynamic range of the measuring equipment; a typical value is 20 dB below the peak level of the delay profile.

FIGURE 3A

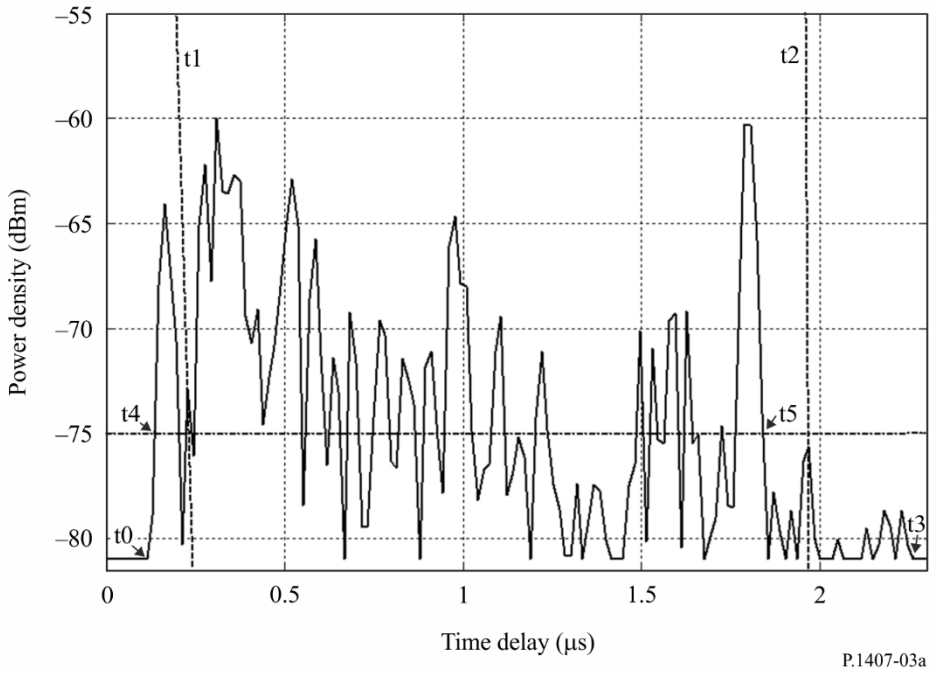

Power delay profile illustrating the following parameters: the delay window, W_{90}, containing 90% of the received power is marked between the two vertical dashed lines (t_1 and t_2), the delay interval, I_{15}, containing the signal above the level 15 dB below the peak, lies between t_4 and t_5. t_0 and t_3 indicate the start and the end of the profile above the noise floor.

FIGURE 3B

Power delay profile indicating multipath components above threshold level

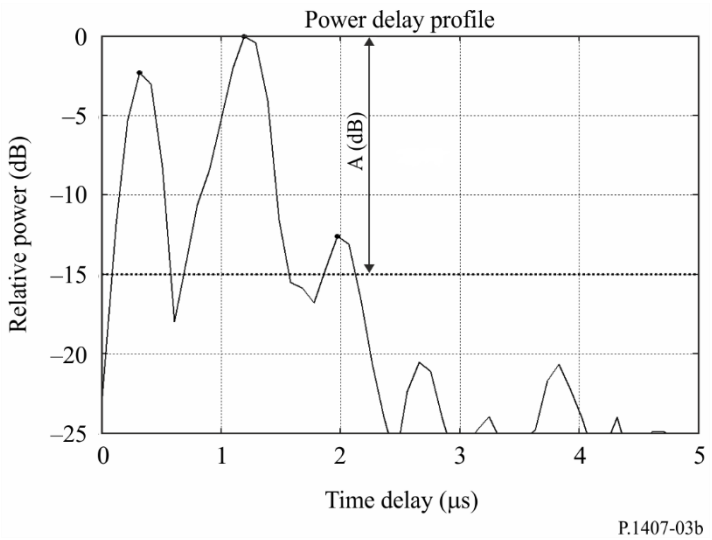

3 Parameters of direction of arrival

Figure 4 shows azimuth angle of arrival θ_h and elevation angle of arrival θ_v.

FIGURE 4

Azimuth angle of arrival θ_h and elevation angle of arrival θ_v

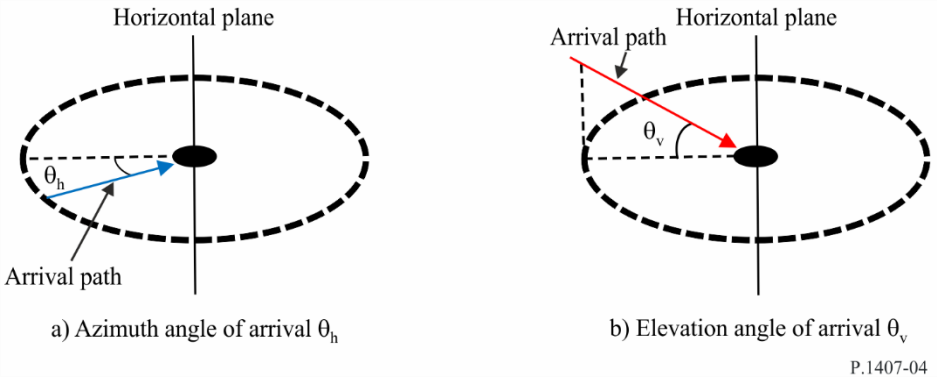

3.1 Definition of azimuth or elevation angle of arrival power profiles

The appropriate parameters for the statistical description regarding the azimuth or elevation angle of arrival of the multipath can be computed from any of three types of azimuth or elevation angle of arrival power profiles: instantaneous azimuth or elevation angle of arrival power profile; short-term azimuth or elevation angle of arrival power profile; or long-term azimuth or elevation angle of arrival power profile, which are either time averages obtained when the receiver is stationary and represent variations in the environment, or spatial averages obtained when the receiver is in motion.

Definitions of azimuth angle of arrival power profiles are given as shown in Fig. 5(a). Definitions of elevation angle of arrival power profiles are given as shown in Fig. 5(b).

FIGURE 5

Definition of the azimuth or elevation angle of arrival power profiles

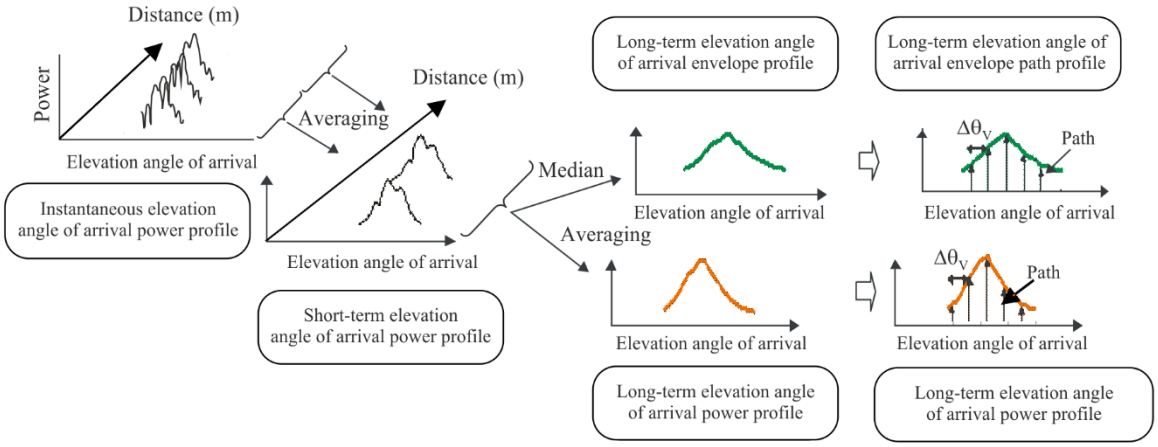

a) Definition of the azimuth angle of arrival power profiles

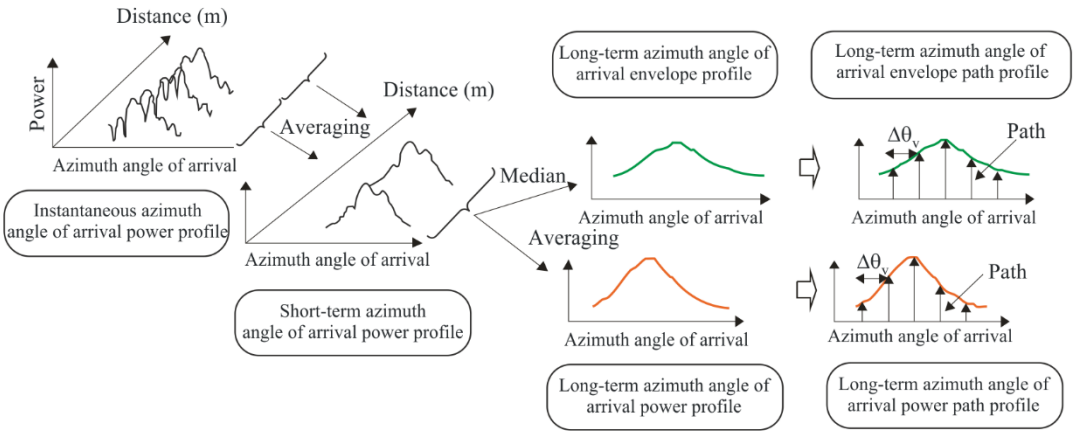

b) Definition of the elevation angle of arrival power profiles

P.1407-05

The instantaneous azimuth or elevation angle of arrival power profile is the power density of the impulse response at one moment at one point.

The short-term azimuth or elevation angle of arrival power profile is obtained by spatially averaging the instantaneous azimuth or elevation angle of arrival power profiles over several tens of wavelengths within the range where the same multipath components are maintained in order to suppress the variations due to rapid fading.

The long-term azimuth or elevation angle of arrival power profile is obtained by spatially averaging the short-term azimuth or elevation angle of arrival power profiles at approximately the same distance from the base station (BS) in order to suppress the variation due to shadowing.

Long-term azimuth or elevation angle of arrival power profiles with a discrete azimuth or elevation angle normalized by the azimuth or elevation angular resolution of the antenna are defined as long-term azimuth or elevation angle of arrival power path profiles, instead of continuous azimuth or elevation angle of arrival power profiles.

On the other hand, the long-term azimuth or elevation angle of arrival envelope profile is the median value of the short-term azimuth or elevation angle of arrival power path profiles at approximately the same distance from the base station, and characterizes the shape of the azimuth or elevation angle of arrival power profile at the area considered.

3.2 Definitions of statistical parameters

The definitions of the appropriate parameters for the statistical description regarding the multipath azimuth or elevation angle of arrival are given below:

The *average azimuth or elevation angle* of arrival is the power-weighted average of the measured directions of azimuth or elevation arrival and is given by the first moment of the power azimuth or elevation spectrum. (It can also be called the power azimuth or elevation angular profile.)

The azimuth or elevation angle of arrival *power profile* is the azimuth or elevation angular power characteristic within the azimuth or elevation plane.

The *r.m.s. azimuth or elevation angular spread* is the power-weighted standard deviation of the azimuth or elevation direction of arrival and is given by the second moment of the power azimuth or elevation angular profile. It provides a measure of the variability of the mean azimuth or elevation angle of arrival.

The *azimuth or elevation angular window* is the width of the middle portion of the azimuth or elevation angle of arrival power profile containing the defined certain percentage of the total power found in that azimuth or elevation angle of arrival power profile measurement.

The *azimuth or elevation angle interval* (or *azimuth or elevation angular spacing*) is defined as the width of the impulse response (or width of the azimuth or elevation angular profile) between two values of direction of arrival. It marks the first azimuth or elevation angle at which the amplitude of the azimuth or elevation angle of arrival power profile exceeds a given threshold, and the last azimuth or elevation angle at which it falls below that threshold. The threshold used depends on the dynamic range of the measuring equipment: a typical value is 20 dB below the peak level of the azimuth or elevation angle of arrival power profile.

3.2.1 Total power

Let the received power in the azimuth or elevation direction, θ_h, θ_v be $p(\theta_h)$, $p(\theta_v)$.

The *total power, p_{0h} p_{0v}*, of the azimuth or elevation angle of arrival power profile is defined as the power beyond the threshold level L_0 which is set to separate the signal from noise, as shown in Fig. 6.

Total power of azimuth angle of arrival power profile is:

$$p_{0h} = \int_{\theta_{0h}}^{\theta_{3h}} p(\theta_h)\,d\theta_h \tag{8a}$$

Total power of elevation angle of arrival power profile is:

$$p_{0v} = \int_{\theta_{0v}}^{\theta_{3v}} p(\theta_v)\,d\theta_v \tag{8b}$$

where:

θ_h, θ_v : measured from the azimuth or elevation direction of the principal signal (assumed to be stationary within the duration of the measurement) (rad)

$p(\theta_h)$, $p(\theta_v)$: azimuth or elevation angle of arrival power profile above the threshold level L_0; below L_0, $p(\theta_h)$, $p(\theta_v) = 0$

L_0 : level with some margin (3 dB recommended) over the noise floor

θ_{0h}, θ_{0v} : azimuth or elevation angle of arrival when $p(\theta_h)$, $p(\theta_v)$ exceeds the threshold level L_0 for the first time in $\theta_{maxh}(-\pi,\pi)/\theta_{maxv}\left(-\frac{\pi}{2},\frac{\pi}{2}\right)$

θ_{3h}, θ_{3v} : azimuth or elevation angle of arrival when $p(\theta_h)$, $p(\theta_v)$ exceeds the threshold level L_0 for the last time in $\theta_{maxh}(-\pi,\pi),\theta_{maxv}\left(-\frac{\pi}{2},\frac{\pi}{2}\right)$.

In discrete form, equations (8a) and (8b) become as follows.

Total power of azimuth angle of arrival power profile is:

$$p_{0h} = \sum_{i=1}^{N} p(\theta_{ih}) \tag{8c}$$

Total power of elevation angle of arrival power profile is:

$$p_{0v} = \sum_{i=1}^{N} p(\theta_{iv}) \tag{8d}$$

where $i = 1$ and N are the indices of the first and the last samples of the azimuth or elevation angle of arrival power profile above the threshold level, respectively.

FIGURE 6

Total power

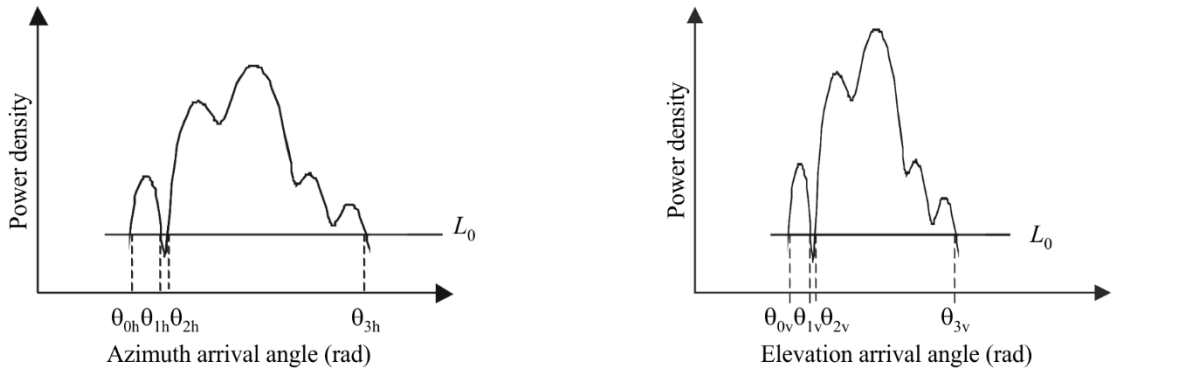

a) Total power of the azimuth angle of arrival power profile

b) Total power of the elevation angle of arrival power profile

P.1407-06

3.2.2 Average azimuth or elevation arrival angle

The average azimuth or elevation angle of arrival, T_{Ah}, T_{Av}, is given by the first moment of the power azimuth or elevation angular profile as follows.

The average azimuth angle of arrival is:

$$T_{Ah} = \frac{1}{p_{0h}} \int_{\theta_{0h}}^{\theta_{3h}} \theta_h p(\theta_h) d\theta_h \tag{9a}$$

The average elevation angle of arrival is:

$$T_{A\nu} = \frac{1}{p_{0\nu}} \int_{\theta_{0\nu}}^{\theta_{3\nu}} \theta_\nu \, p(\theta_\nu) \, d\theta_\nu \tag{9b}$$

In discrete form with azimuth or elevation angular resolution, $\Delta\theta_h$, $\Delta\theta_v$, equations (9a) and (9b) become as follows.

The average azimuth angle of arrival is:

$$T_{Ah} = \frac{\sum_{i=1}^{N} \theta_{ih} \, p(\theta_{ih})}{\sum_{i=1}^{N} p(\theta_{ih})} \tag{9c}$$

$$\theta_{ih} = (i - 1) \, \Delta\theta_h \; (i = 1, 2, \ldots..N)$$

The average elevation angle of arrival is:

$$T_{A\nu} = \frac{\sum_{i=1}^{N} \theta_{i\nu} \, p(\theta_{i\nu})}{\sum_{i=1}^{N} p(\theta_{i\nu})} \tag{9d}$$

$$\theta_{i\nu} = (i - 1) \, \Delta\theta_\nu \; (i = 1, 2, \ldots..N)$$

where $i = 1$ and N are the indices of the first and the last samples of the azimuth or elevation angle of arrival power profile above the threshold level, respectively.

3.2.3 r.m.s. azimuth or elevation angular spread

The r.m.s. azimuth or elevation angular spread, S_{Ah}, $S_{A\nu}$ of the direction of arrival is defined as follows.

The r.m.s. azimuth angular spread is:

$$S_{Ah} = \sqrt{\frac{1}{p_{0h}} \int_{\theta_{0h}}^{\theta_{3h}} (\theta_h - T_{Ah})^2 \, p(\theta_h) \, d\theta_h} \tag{10a}$$

The r.m.s. elevation angular spread is:

$$S_{A\nu} = \sqrt{\frac{1}{p_{0\nu}} \int_{\theta_{0\nu}}^{\theta_{3\nu}} (\theta_\nu - T_{A\nu})^2 \, p(\theta_\nu) \, d\theta_\nu} \tag{10b}$$

In discrete form with azimuth or elevation angular resolution, $\Delta\theta_h$, $\Delta\theta_v$, equations (10a) and (10b) become as follows.

The r.m.s. azimuth angular spread is:

$$S_{Ah} = \sqrt{\frac{\sum_{i=1}^{N} (\theta_{ih} - T_{Ah})^2 \, p(\theta_{ih})}{\sum_{i=1}^{N} p(\theta_{ih})}} \tag{10c}$$

The r.m.s elevation angular spread is:

$$S_{Av} = \sqrt{\frac{\sum_{i=1}^{N} (\theta_{iv} - T_{Av})^2 \, p(\theta_{iv})}{\sum_{i=1}^{N} p(\theta_{iv})}} \tag{10d}$$

where $i = 1$ and N are the indices of the first and the last samples of the angle of arrival power profile above the threshold level, respectively.

3.2.4 Azimuth or elevation angular window

The azimuth or elevation angular window, θ_{wh}, θ_{wv}, is the width of the middle portion of the azimuth or elevation angle of arrival power profile containing a percentage q, of the total power as shown in Fig. 7.

The azimuth angular window is:

$$\theta_{wh} = \theta_{w2h} - \theta_{w1h} \tag{11a}$$

The elevation angular window is:

$$\theta_{wv} = \theta_{w2v} - \theta_{w1v} \tag{11b}$$

whereby the boundaries, θ_{w1h}, θ_{w1v} and θ_{w2h}, θ_{w2v} are defined as follows.

θ_{w1h} and θ_{w2h} are:

$$\int_{\theta_{w1h}}^{\theta_{w2h}} p(\theta_h) \, d\theta_h = \frac{q}{100} \int_{\theta_{0h}}^{\theta_{3h}} p(\theta_h) \, d\theta_h = \frac{q}{100} \, p_{0h} \tag{12a}$$

θ_{w1v} and θ_{w2v} are:

$$\int_{\theta_{w1v}}^{\theta_{w2v}} p(\theta_v) \, d\theta_v = \frac{q}{100} \int_{\theta_{0v}}^{\theta_{3v}} p(\theta_v) \, d\theta_v = \frac{q}{100} \, p_{0v} \tag{12b}$$

and the power outside of the window is split into two equal parts $\left(\frac{100-q}{200}\right) p_{0h}$, $\left(\frac{100-q}{200}\right) p_{0v}$.

FIGURE 7

Azimuth or elevation angular window

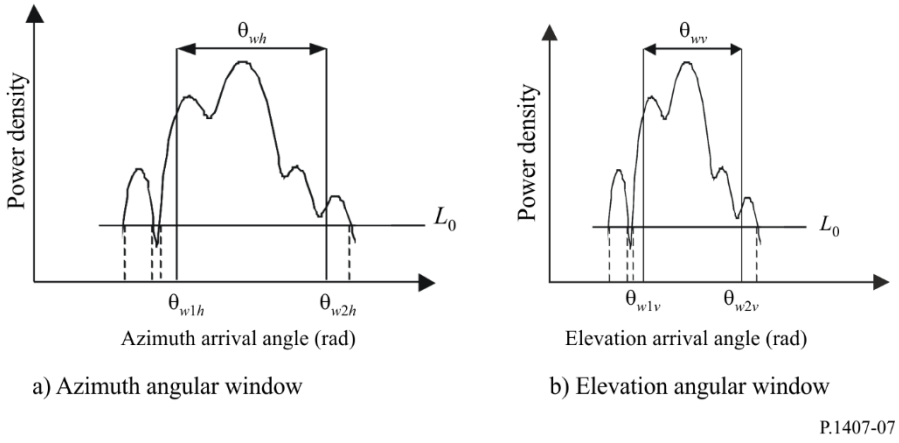

3.2.5 Azimuth or elevation angle interval (azimuth or elevation angular spacing)

The azimuth or elevation angle interval, A_{thh}, A_{thv}, is defined as the azimuth or elevation angle difference between the angle, θ_{4h}, θ_{4v} when the amplitude of the azimuth or elevation angle of arrival power profile first exceeds a given threshold, L_{th}, and the azimuth or elevation angle, θ_{5h}, θ_{5v} when it falls below that threshold for the last time as shown in Fig. 8.

The azimuth angle interval is:

$$A_{thh} = \theta_{5h} - \theta_{4h} \tag{13a}$$

The elevation angle interval is:

$$A_{th\nu} = \theta_{5\nu} - \theta_{4\nu} \tag{13b}$$

FIGURE 8

Azimuth or elevation angle interval

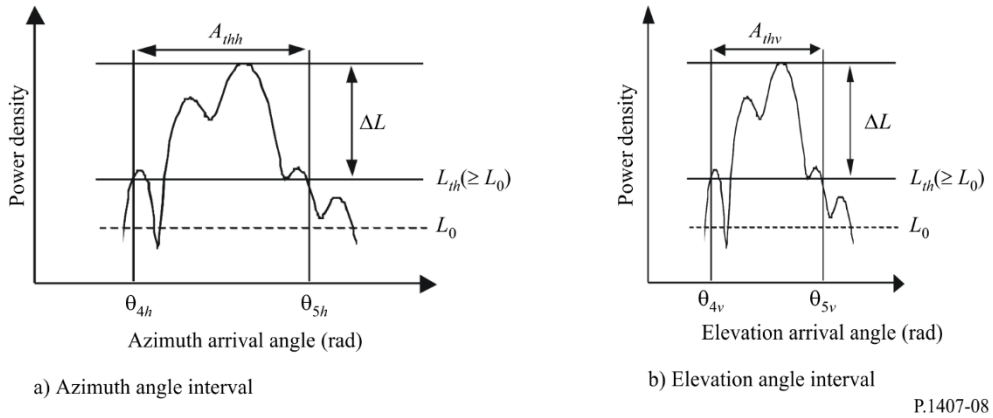

3.2.6 Spatial correlation distance

In particular for multiple-output multiple-input (MIMO) channels, the spatial correlation coefficient for different spacing d is obtained from the azimuth or elevation angle variant complex transfer

function of the power azimuth or elevation angular profile. The spatial correlation coefficient of azimuth or elevation angle, $R_h(d)$, $R_v(d)$, is defined as follows.

The spatial correlation coefficient of azimuth angle is:

$$R_h(d) = \frac{\int_{\theta_{0h}}^{\theta_{3h}} p(\theta_h) \exp(-j2\pi d \sin\theta_h / \lambda) d\theta_h}{\int_{\theta_{0h}}^{\theta_{3h}} p(\theta_h) d\theta_h} \tag{14a}$$

The spatial correlation coefficient of elevation angle is:

$$R_v(d) = \frac{\int_{\theta_{0v}}^{\theta_{3v}} p(\theta_v) \exp(-j2\pi d \sin\theta_v / \lambda) d\theta_v}{\int_{\theta_{0v}}^{\theta_{3v}} p(\theta_v) d\theta_v} \tag{14b}$$

where:

d : distance for different spacing

λ : wavelength.

As shown in Fig. 9, the spatial correlation distance d_c is defined as the first-cut off distance at which $|R_h(d)|$, $|R_v(d)|$ equals x% of $|R_h(d = 0)|$, $|R_v(d = 0)|$.

The spatial correlation distance of azimuth angle is:

$$|R_h(d_c)| / |R_h(0)| = x / 100 \tag{15a}$$

The spatial correlation distance of elevation angle is:

$$|R_v(d_c)| / |R_v(0)| = x / 100 \tag{15b}$$

FIGURE 9

Spatial correlation distance

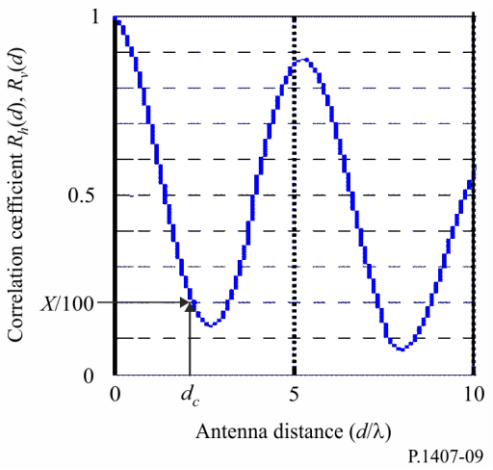

3.2.7 Recommended parameters

Azimuth or elevation angular windows for 50%, 75% and 90% power, azimuth or elevation angle intervals for thresholds of 9, 12 and 15 dB below the peak, and correlation distances for 50% and 90% of correlation are recommended to permit a detailed analysis of data. Furthermore, it is worth noting that the effects of noise and spurious signals in the system (from RF to data processing) can be very significant. Therefore, it is important to determine the noise and/or spurious threshold of the systems accurately and to provide a safety margin on top of that. A safety margin of 3 dB is recommended, and in order to ensure the integrity of results, it is recommended that a minimum peak-to-spurious ratio of, for example, 15 dB (excluding the 3 dB safety margin) be used as an acceptance criterion limiting the azimuth or elevation angle of arrival power profiles included in the statistics. Figure 10 shows an example of the effect of setting the magnitude of minimum peak-to-L_{th} ratio (ΔL). In this Figure, the azimuth or elevation angle of arrival power profile is assumed to be a Laplace distribution (double exponential distribution**)** with azimuth or elevation angular spread of 14 degrees; azimuth or elevation angular spread and azimuth or elevation angular interval are calculated as functions of the peak power-to-L_{th} ratio. This Figure shows that these parameters undergo significant changes even for essentially identical values. Therefore the value used as ΔL in the statistical evaluation should be specified.

FIGURE 10

Example of effect for minimum peak-to-L_{th} ratio (ΔL)

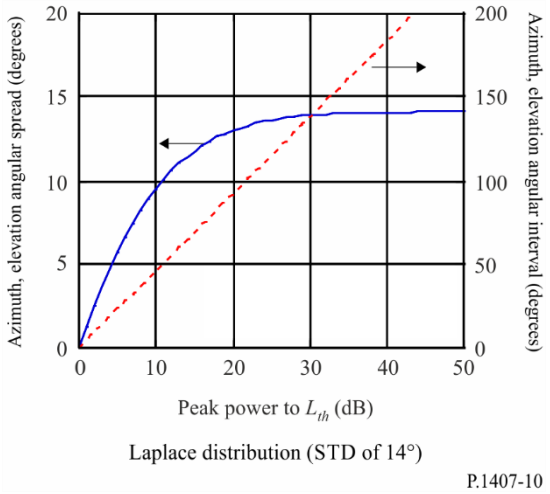

4 Parameters of directional power-delay profile

The power angle-delay profile is obtained from directional measurements giving the received power as a function of angle of arrival as a function of time delay as illustrated in Fig. 11.

FIGURE 11

Directional power delay profiles

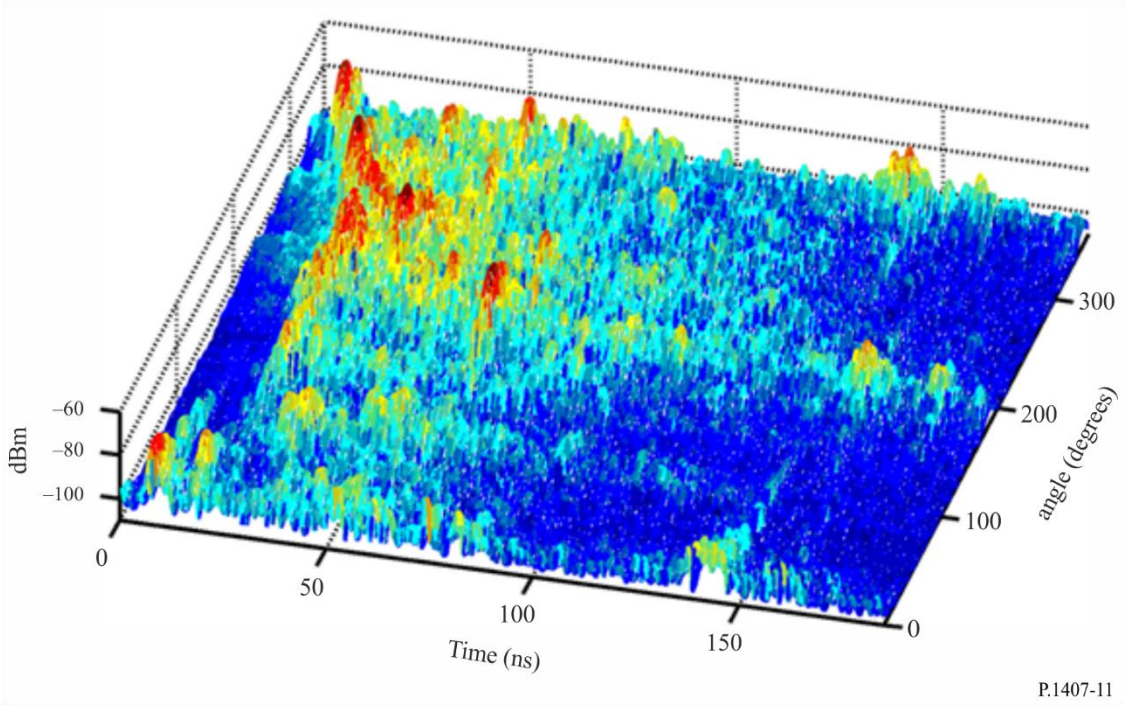

The omni-directional power delay profile as a function of time delay can be obtained from the sum of the power delay profiles over all angles. The *total omni-directional power*, is given in equation (16) when synthesized from directional measurements:

$$p_m = \int_{\theta_{0v}}^{\theta_{3v}} \int_{\theta_{0h}}^{\theta_{3h}} \int_{t_0}^{t_3} p(t,\theta_h,\theta_v)\,dt\,d\theta_h\,d\theta_v - G_A \qquad (16)$$

where:

$p(t)$: power density of the impulse response in linear units of power obtained with omni-directional antennas

$p(t,\theta_h,\theta_v)$: directional power density of the impulse response in linear units of power

t : delay with respect to a time reference

t_0 : instant when $p(t)$ or $p(t,\theta_h,\theta_v)$ exceeds the cut-off level for the first time

t_3 : instant when $p(t)$ or $p(t,\theta_h,\theta_v)$ exceeds the cut-off level for the last time

θ_{0h} : azimuth angle when $p(t,\theta_h,\theta_v)$ exceeds the cut-off level for the first angle

θ_{3h} : azimuth angle when $p(t,\theta_h,\theta_v)$ exceeds the cut-off level for the last angle

θ_{0v} : elevation angle when $p(t,\theta_h,\theta_v)$ exceeds the cut-off level for the first angle

θ_{3v} : elevation angle when $p(t,\theta_h,\theta_v)$ exceeds the cut-off level for the last angle

G_A : antenna gain due to incremental angular steps below the 3 dB beamwidth which results in an overlap of the antenna beam which leads to an increase in the received power by G_A

For each angle of arrival, time delay parameters in §§ 2.2.2 to 2.2.6 can be computed.

5 Parameters of the received signal variations

5.1 Definition of the received signal variations as a function of time and frequency

The variations of the received signal in time and in frequency can be measured from: periodically sweeping across the frequency band of interest over a short time interval, or from the Fourier transform of the short-term impulse responses. The resulting small scale time variant frequency response H(*f*,*t*) illustrated in Fig. 12 can be used to generate the covariance function of the channel $R_H(f, f';t,t')$ as in equation (17) where *E* is the expectation:

$$R_H(f, f';t,t') = E\{H(f,t)H*(f',t')\} \tag{17}$$

Under the assumption of wide sense stationary uncorrelated scattering (WSSUS), the covariance function in equation (17) becomes a function of the difference in frequency, Δf, and difference in time, Δt, $R_H(\Delta f, \Delta t)$.

The degree of correlation is expressed by the normalized spaced-frequency spaced-time function, given by equation (18).

$$\rho(\Delta f,\Delta t) = \frac{R_H(\Delta f,\Delta t)}{\sqrt{E\left[|H(f,t)|^2\right]E\left[|H(f+\Delta f,t+\Delta t)|^2\right]}} \tag{18}$$

Parameters related to the covariance function in equation (17) and H(*f*,*t*) are defined in § 5.2.

FIGURE 12

Small scale time variant frequency function

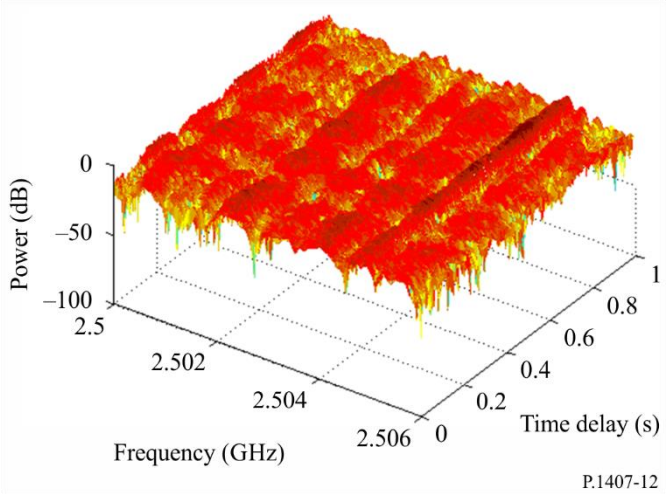

5.2 Definitions of statistical parameters

5.2.1 Coherent bandwidth or frequency correlation

For WSSUS channels which have a dominant multipath component, the coherent (correlation) bandwidth is obtained from equation (19a). For power delay profiles which exhibit a significant structure of multipath, the coherent bandwidth can be estimated from the Fourier transform $C(f)$ of the power density of the impulse response $p(\tau)$ as in equation (19b):

$$R_H(\Delta f) = R_H(\Delta f,\Delta t)\big|_{\Delta t=0} \tag{19a}$$

$$C(f) = \int_0^{\tau_e} p(\tau)\exp(-j2\pi f\tau)d\tau \tag{19b}$$

The correlation bandwidth, B_x, is defined as the frequency for which $|R_H(\Delta f)|$ or $|C(f)|$ equals x% of $R_H(\Delta f = 0)$ or $C(f = 0)$.

5.2.2 Coherent time or time correlation

For WSSUS, the coherent time is estimated from the time correlation of the channel as in equation (20).

$$R_H(\Delta t) = R_H(\Delta\omega, \Delta t)\big|_{\Delta\omega=0} \tag{20}$$

The coherent time, T_x, is defined as the time interval for which $|R_H(\Delta t)|$ equals x% of $|R_H(\Delta t = 0)|$.

5.2.3 Level crossing rate and average fade duration

The level crossing rate (LCR) and average fade duration (AFD) are obtained from the received signal strength variations at a single frequency as a function of time or distance or from the amplitude of the time variant frequency function at a single frequency measured as a function of time or distance. For a given time interval, the LCR is the number of times the received signal crosses a particular level, whereas the AFD is the duration of time it spends below the specified level. For example for a level of −12.5 dB, Fig. 13 illustrates the LCR and the AFD where the double arrows indicate the time that the signal remains below the level and the vertical arrows indicate the times at which the specified level is crossed in the positive going direction.

FIGURE 13

Received signal strength versus time

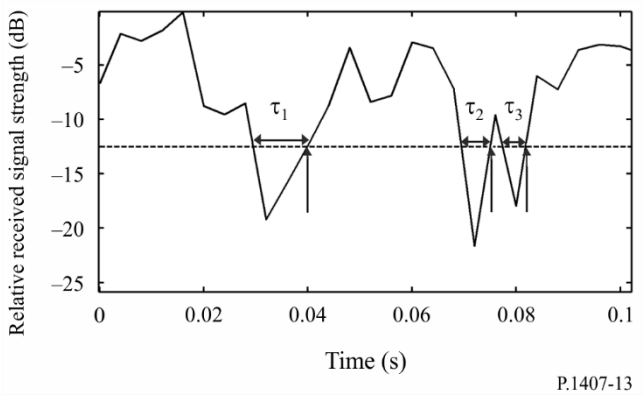

5.2.4 Level crossing frequency and average fade bandwidth

The level crossing frequency (LCF) and average fade bandwidth (AFBW) are obtained from the received signal strength variations as a function of frequency or from the amplitude of the time variant frequency function at a single instant in time, as in Fig. 13 where the time axis is replaced by the frequency axis. For a given bandwidth, the LCF is the number for which the received signal crosses a particular level and the AFBW is the average frequency range that falls below the specified threshold level. Figure 14 illustrates the two parameters computed for threshold levels between −15 dB to 0 dB.

FIGURE 14

Normalized average fade bandwidth and level crossing frequency

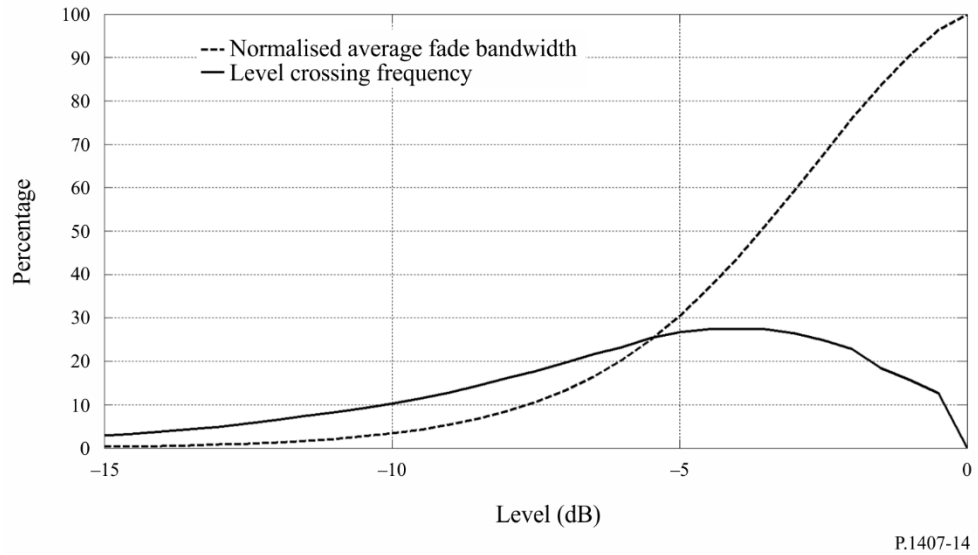

5.2.5 Recommended parameters

The *correlation bandwidth* is defined as the band of frequencies for which the autocorrelation function of the transfer function is above a given threshold; typical threshold values are 0.5 and 0.9. The LCR is usually estimated for the number of level crossings per second and the LCF is the number of level crossings per MHz.

6 Specific case of narrow band modelling

In the very specific case when the signal bandwidth is smaller than the coherence bandwidth of the channel, the modelling process may be simplified to flat fading as illustrated in Fig. 15, where all frequencies inside the signal bandwidth will be similarly impacted.

FIGURE 15

Narrow band principle

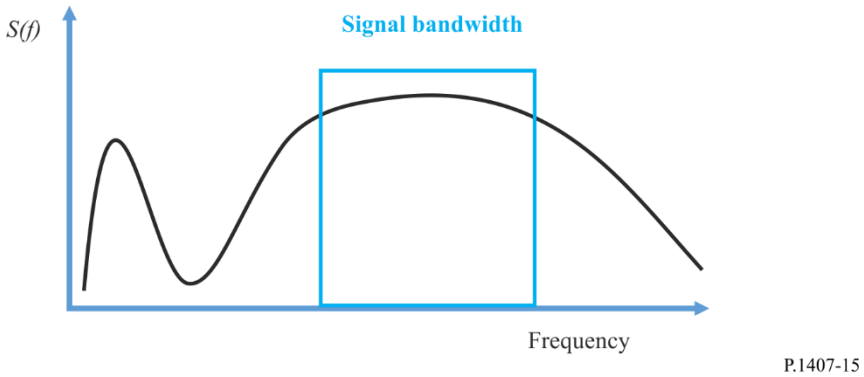

In contrast to the wideband channel where the received signal y(t) can be expressed as in equation (21):

$$y(t) = \sum_{n=1}^{N} \gamma_n(t) s\left(t - \tau_n(t)\right) exp(-i2\pi f_{d,n}(t)) \quad (21)$$

where:

$s(t)$: transmitted signal

N : number of multipath components

$\gamma_n(t)$: n^{th} multipath component amplitude

$\tau_n(t)$: time delay

$f_{d,n}(t)$: Doppler shift.

In the case of the narrow band assumption, equation (21) can be simplified to:

$$y(t) = s(t)\sum_{n=1}^{N}\gamma_n(t)\exp\left(-j2\pi f_{d,n}t\right) \tag{22}$$

$$y(t) = s(t)a(t) \tag{23}$$

where $a(t)$ is a time series that models the signal attenuation which can be modelled by a stochastic process defined by two components: a statistical model and a spectrum model.

In the case of terrestrial applications, Rayleigh or Rice distribution probability density functions as in Recommendation ITU-R P.1057 can be used in conjunction with Jake's Doppler spectrum given by:

$$\begin{cases} S(f) = \dfrac{K}{\pi f_m\sqrt{1-\left(\frac{f}{fm}\right)^2}}\ for\ |f| < f_m \\ S(f) = 0\ else \end{cases} \tag{24}$$

where the maximum Doppler frequency $f_m = v_m \times f/c$ and K is a normalisation parameter which ensures that the filtering does not change the process power, v_m is the receiver speed, f is the carrier frequency and c is the speed of light.

For Earth-space transmission, the attenuation distribution and spectrum model are given in Recommendation ITU-R P.681.

7 Test for stationary distance

The stationary distance is the distance over which the channel can be considered to be wide sense stationary. To determine the stationary distance, apply the Run test to consecutive impulse responses by dividing the data set into equal N_i groups containing the same number of impulse responses, obtained over spatial distances which are less than $c \times \Delta t$ where Δt is the time delay resolution of the power delay profile (PDP) and c is the speed of light. The PDPs are then used to estimate the rms delay spread. The median rms delay spread is estimated and each rms value is designated by + sign or – sign if it falls above or below the median value respectively (numbers equal to the median are removed). Consecutive + signs or – signs are counted as a single positive N_+ or negative N_- run. The total number of runs N_{runs}, is the sum of the number of positive and negative runs:

$$N_{runs} = N_+ + N_-$$

N_{runs} of a sequence of +++------+++ is equal to three with two positive Runs N_+ and one negative Run N_-.

Subsequently, $n = N_i/2$ is entered into Table 1 to identify the acceptable low and high number of Runs for low and high confidence levels, c_{low} and c_{high}, respectively. Check if the number of computed runs N_{runs} falls outside these limits, as given in equation (25).

$$\text{check if } \left[c_{low} \le N_{runs} \le c_{high} \middle| N_i\right] \tag{25}$$

For confidence levels of 0.05 and 0.95, check if

$$c_{0.05} \leq N_{runs} \leq c_{0.95} \quad (26)$$

If N_{runs} falls outside these limits, average over a different number of impulse responses until the Run test gives the stationary distance, which is the distance travelled during N_i impulse responses.

TABLE 1

N	0.99	0.975	0.95	0.05	0.025	0.01
5	2	2	3	8	9	9
6	2	3	3	10	10	11
7	3	3	4	11	12	12
8	4	4	5	12	13	13
9	4	5	6	13	14	15
10	5	6	6	15	15	16
11	6	7	7	16	16	17
12	7	7	8	17	18	18
13	7	8	9	18	19	20
14	8	9	10	19	20	21
15	9	10	11	20	21	22
16	10	11	11	22	22	23
18	11	12	13	24	25	26
20	13	14	15	26	27	28
25	17	18	19	32	33	34
30	21	22	24	37	39	40
35	25	27	28	43	44	46
40	30	31	33	48	50	51
45	34	36	37	54	55	57
50	38	40	42	59	61	63
55	43	45	46	65	66	68
60	47	49	51	70	72	74
65	52	54	56	75	77	79
70	56	58	60	81	83	85
75	61	63	65	86	88	90
80	65	68	70	91	93	96
85	70	72	74	97	99	101
90	74	77	79	102	104	107
95	79	82	84	107	109	112
100	84	86	88	113	115	117

Annex 2

1 Introduction

This Annex illustrates some results of computing the correlation coefficients from a power angular profile and the effect of the correlation coefficients on MIMO capacity.

2 Computing the spatial correlation coefficients

The definition in equation (14) of Annex 1 has been used to compute the spatial correlation. This Annex briefly introduces a result and illustrates how the correlation is affected by antenna spacing.

Figure 16 shows an ideal truncated Laplacian power-azimuth spectrum (PAS) such as:

$$PAS_L(\varphi) = \sum_{k=1}^{N_c} \frac{Q_{L,k}}{\sigma_{L,k}\sqrt{2}} \exp\left[-\frac{\sqrt{2}|\varphi - \varphi_{0,k}|}{\sigma_{L,k}}\right] \left\{\varepsilon\left[\varphi - (\varphi_{0,k} - \Delta\varphi_k)\right] - \varepsilon\left[\varphi - (\varphi_{0,k} + \Delta\varphi_k)\right]\right\} \quad (27)$$

where:

$\varepsilon(\varphi)$: step function

N_c : number of clusters

$\varphi_{0,k}$: mean angle of incidence of k-th cluster

$\sigma_{L,K}$: angular spread.

PAS is defined over $[\varphi_0 - \Delta\varphi, \varphi_0 + \Delta\varphi]$. The power normalization condition is assumed as:

$$\sum_{k=1}^{N_c} Q_{L,k}\left[1 - \exp\left(-\frac{\sqrt{2}\Delta\varphi_k}{\sigma_{L,k}}\right)\right] = 1 \quad (28)$$

Then the envelope correlation coefficient is given by:

$$\rho_e(D) = \left|R_{XX}(D) + jR_{XY}(D)\right|^2 \quad (29)$$

where:

$D = 2\pi d/\lambda$

D : antenna spacing

λ : wavelength,

and the cross-correlation functions $R_{XX}(D)$ and $R_{XY}(D)$ are defined in equation (15).

FIGURE 16

Ideal truncated Laplacian power-azimuth spectrum (PAS)

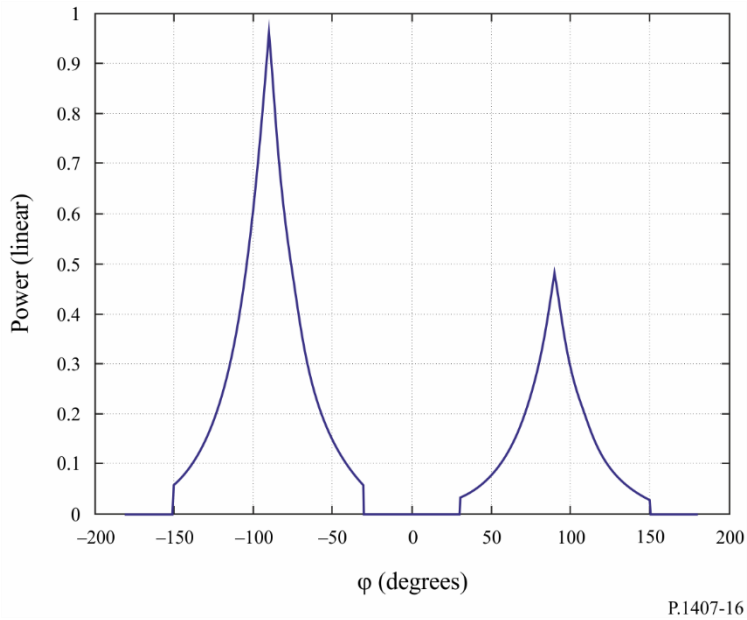

Normalized Laplacian PAS for a two-cluster case. $AS = 30°$, $\varphi_0 \in [-90^\circ, +90^\circ]$. Additionally, the +90º cluster has half the power of the –90º case.

Figure 17 illustrates the resulting spatial correlation.

FIGURE 17

Resulting spatial correlation

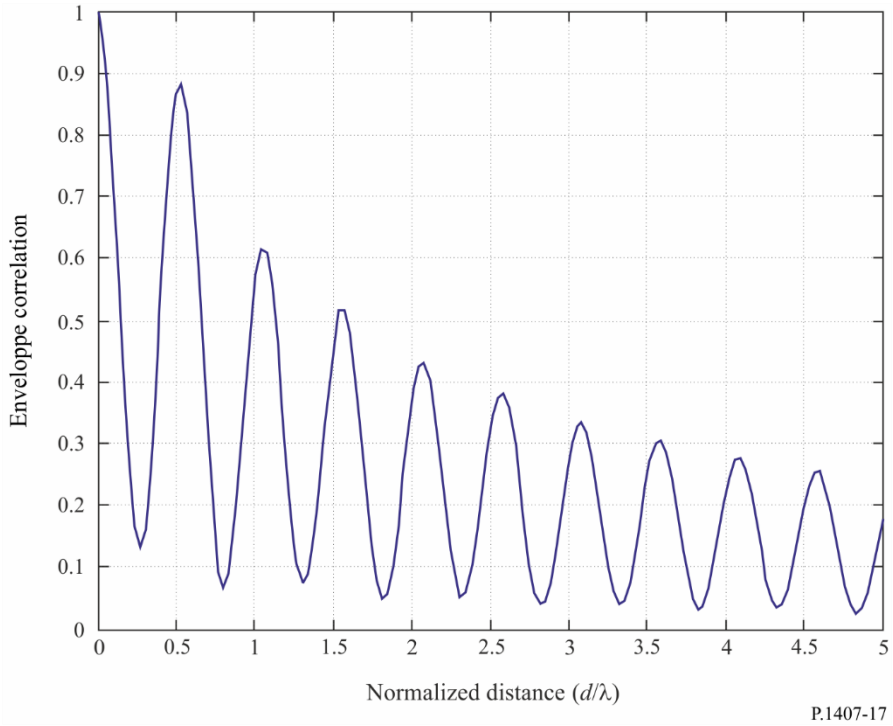

Envelope correlation coefficient versus the normalized distance = d/λ for the two-cluster case shown in Fig. 16.

3 Effect of the correlation coefficients on MIMO capacity

For Rayleigh fading channels, the ergodic MIMO capacity without channel knowledge at the transmitter is:

$$C = \log_2 \det\left(I_{n_R} + \frac{p}{n_T \sigma^2} R_R^{1/2} H_w R_T H_w^H \left(R_R^{1/2}\right)^H \right) = \log_2 \det\left(I_{n_R} + \frac{p}{n_T \sigma^2} H_w R_T H_w^H R_R^H \right) \quad (30)$$

where:

n_R : number of receiver antennas

n_T : number of transmitter antennas

p : average received power per antenna

σ^2 : noise power at each receive antenna

I_{n_R} : $n_R \times n_R$ identity matrix

$(\cdot)^H$ and $\det(\cdot)$: Hermitian and determinant operation, respectively

H_w : matrix whose elements are independent identically-distributed complex Gaussian Random variables with zero mean and unit variance

$(\cdot)^{½}$: Hermitian square root of a matrix.

The matrices R_R and R_T determine the spatial correlations between the receivers and the transmitters, respectively, where the channel matrix H is defined by $H = R_R^{1/2} H_w R_T^{1/2}$, $R_R^{1/2}$, and $R_T^{1/2}$ are positive definite Hermitian matrices, and finally they are assumed to be normalized such that $[R_R]_{j,j}$ for $j = 1, K, n_R$ and $[R_T]_{i,i}$ for $i = 1, K, n_T$.

By assuming that R_R and R_T have full rank and $n_R = n_T = n$, then at high S/N (p/σ^2) the capacity can be approximated as:

$$C \approx \log_2 \det\left(\frac{p}{n_T \sigma^2} H_w H_w^H \right) + \log_2 \det(R_R) + \log_2 \det(R_T) \quad (31)$$

If the eigenvalues of R_R are denoted by λ_i, $i = 1, K, n$, then $\sum_{i=1}^{n} \lambda_i = n$. From the arithmetic mean-geometric mean inequality:

$$\prod_{i=1}^{n} \lambda_i \le 1 \quad (32)$$

Since $\det(R_R) = \prod_{i=1}^{n} \lambda_i$, it follows that $\log_2 \det(R_R) \le 0$, and is zero only if all eigenvalues of R_R are equal, i.e., $R_R = I_n$. Thus, the correlation determines the MIMO capacity and the loss in the ergodic capacity at high S/N is given by ($\log_2 \det(R_R) + \log_2 \det(R_T)$) bit/s/Hz.

Figure 18 illustrates the effect of spatial correlations on the ergodic capacity of a MIMO channel with $n_R = n_T = 2$. In the Figure, $R_T = I_2$, is assumed. The receiver correlation matrix is chosen according to:

$$R_R = \begin{bmatrix} 1 & \rho_R \\ \rho_R^* & 1 \end{bmatrix} \quad (33)$$

where ρ_R denotes the spatial correlation between the receive antennas.

FIGURE 18

Ergodic capacity with low and high receive correlation

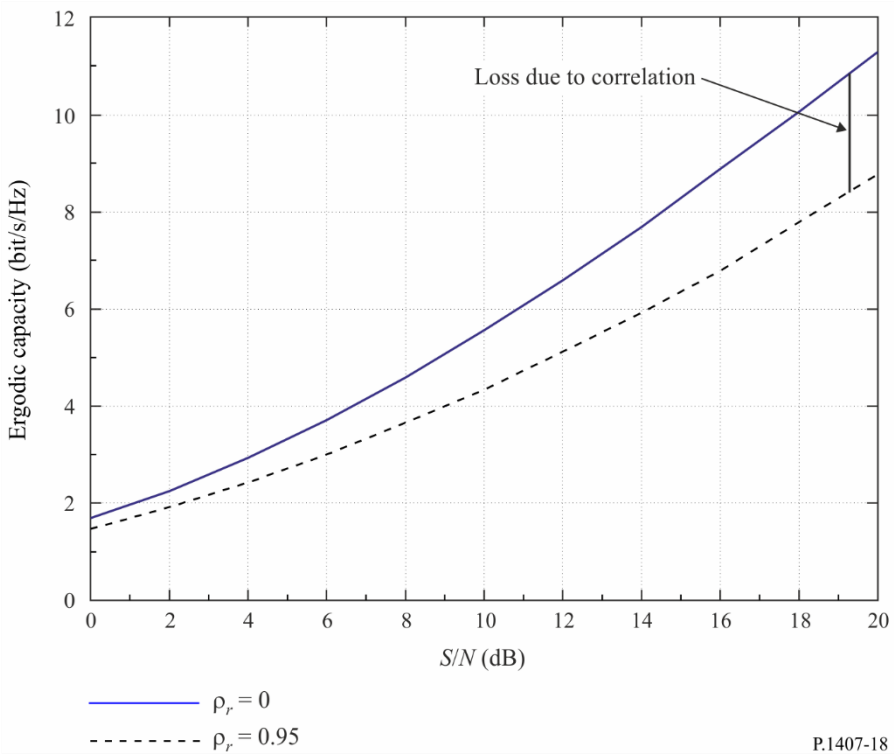

Annex 3

1 Introduction

The resolution of multipath components in measured data depends on the bandwidth of the waveform used in the measurements. The unresolved multipath components give rise to signal variations in time or in space due to the movement of either the transmitter or receiver or changes in the environment as illustrated in Fig. 1. These variations can be modelled by probability density functions such as Rayleigh and Rice as given in Recommendation ITU-R P.1057.

2 Generation of wideband channel

The time variant impulse response can be used to model the channel as a tapped delay line as in Fig. 19 where each tap is delayed by $\Delta\tau$ which corresponds to the time delay resolution of multipath and a tap coefficient which represents the time variations of the unresolved group of multipath components in that time delay interval.

FIGURE 19

Example of multipaths used to generate the channel

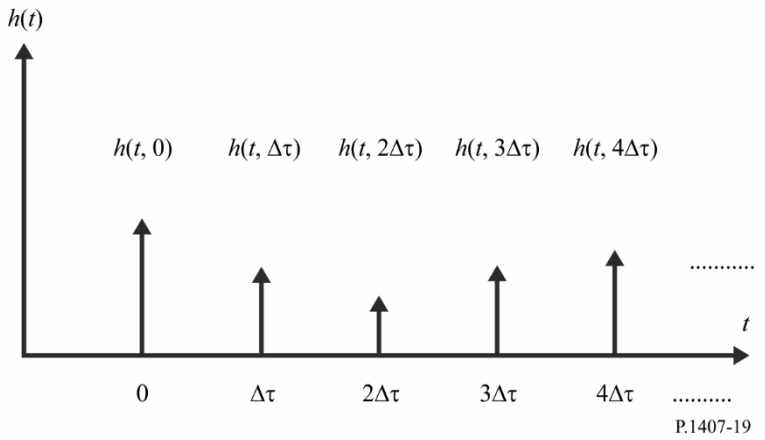

For system simulation, it is sufficient to replace the many scattered paths that may exist in a real channel with only a few $m=n+1$ multipath components in the model as in Fig. 20. This gives the channel response *h(t)* in equation (34):

$$h(t) = \sum_{i=0}^{n} h_i \delta(t - i\Delta\tau) \tag{34}$$

FIGURE 20

Tapped delay line model of multipath

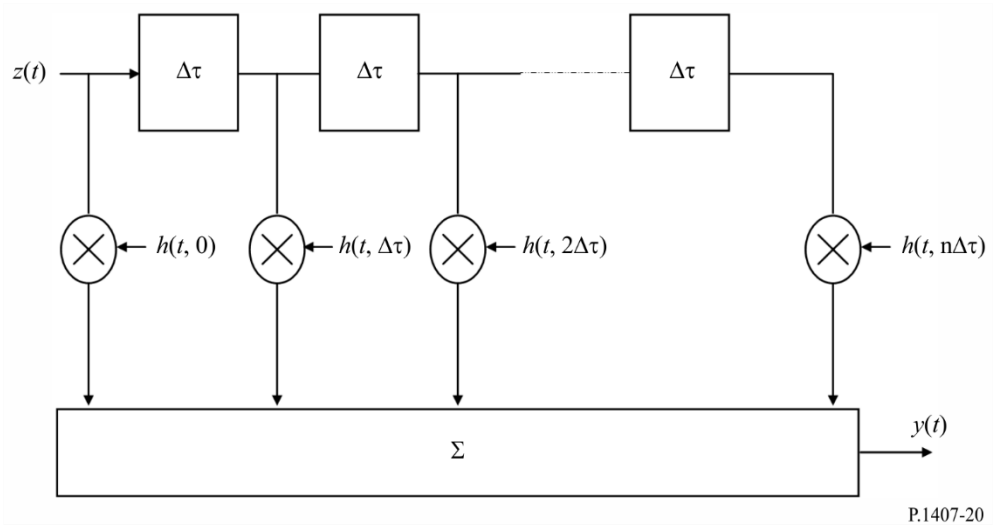

For time delays which have a dominant or line-of-sight (LOS) component, the channel model for each group of multipath components is given by a Rician probability density function. When the Rice factor, *K*, is equal to zero, the Rayleigh model can be used. The generalized channel model is given in equation (35):

$$h(t) = \sum_{i=0}^{n} \left\{ \sqrt{\frac{K_i p_i}{K_i + 1}} e^{j(2\pi f_{o,i} t + \varphi_{o,i})} + \sqrt{\frac{p_i}{K_i + 1}} g_i(t) \right\} \delta(t - i\Delta\tau) \tag{35}$$

where:

K_i : Rician *K*-factor for the i^{th} component defined as the ratio of the power of the dominant or LOS component to the scattered component. When $K_i = 0$, the resulting distribution is Rayleigh

p_i : averaged power of the i^{th} component in *h(t)* and is equal to $p_i = E\left[\left|h_i(t)\right|^2\right]$

$f_{o,I}$: Doppler frequency of the dominant or LOS component of the i^{th} component in *h(t)* and is equal to $F_{D\max,i}\cos\theta_{o,i}$ where $f_{D\max,i}$ is the maximum Doppler shift and $\theta_{o,i}$ is the azimuthal angle of arrival

$\varphi_{o,I}$: initial phase of the LOS component of the i^{th} component in *h(t)*

$g_i(t)$: unit power, zero-mean, complex signal representing the diffuse scattering components. For large number of scatters, $g_i(t)$ can be treated as a complex Gaussian random process with unit variance passed through the i^{th} Doppler filter.

3 Generation of narrowband channel

The time series of a narrowband channel can be generated by the Sum of Sinusoids (SoS) model given in equation (36), which can be associated with any Doppler spectrum model, where each multipath component can be written as a sum of sinusoids.

$$\mu(t) = \mu_1(t) + j\mu_2(t) \tag{36}$$

where $\mu_i(t)$ are two independent stochastic processes as given in equations (37) and (38) and illustrated in Fig. 21.

$$\mu_1(t) = \sum_{n=1}^{N} c_n^{Re}\cos(2\pi f_n^{Re}t + \theta_n^{Re}) \tag{37}$$

$$\mu_2(t) = \sum_{n=1}^{N} c_n^{Im}\sin(2\pi f_n^{Im}t + \theta_n^{Im}) \tag{38}$$

FIGURE 21

Sum of Sinusoid principle

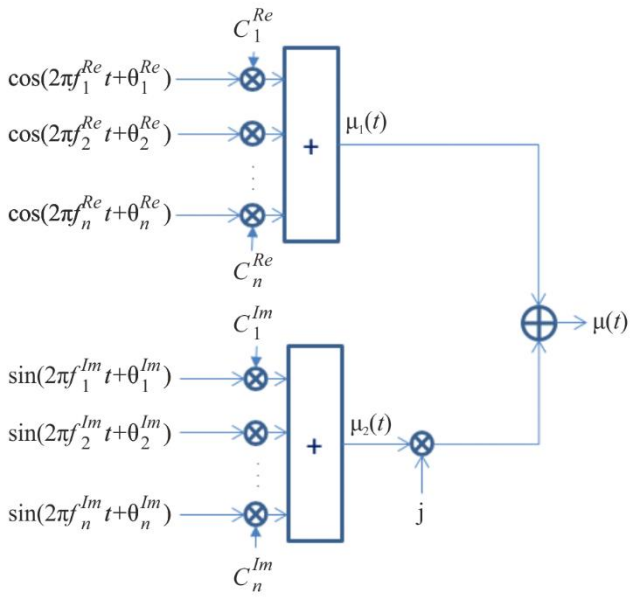

P.1407-21

where θ_n^{Re} and θ_n^{Im} are independent and uniform random processes over 2π, c_n^{Re}, c_n^{Im} and f_n^{Re}, f_n^{Im} are coefficients which must be tuned for the input spectrum and N is the number of sinusoids, (recommended number, N = 50). The coefficients, are estimated with the following two steps:

Step 1: The frequencies f_n^{Re} and f_n^{Im} are randomly selected from a (uniform distribution) between $[-f_{max}, f_{max}]$ with $f_{max} = \frac{v}{\lambda}$

Step 2: c_n^{Re} and c_n^{Im} are estimated by integration of the reference spectrum between $\left[f_n^{Re} - \frac{f_n^{Re} - f_{n-1}^{Re}}{2}, f_n^{Re} + \frac{f_{n+1}^{Re} - f_n^{Re}}{2}\right]$.

An example is shown in Fig. 22.

FIGURE 22

Doppler spectrum estimation (Step 1 and 2) principle

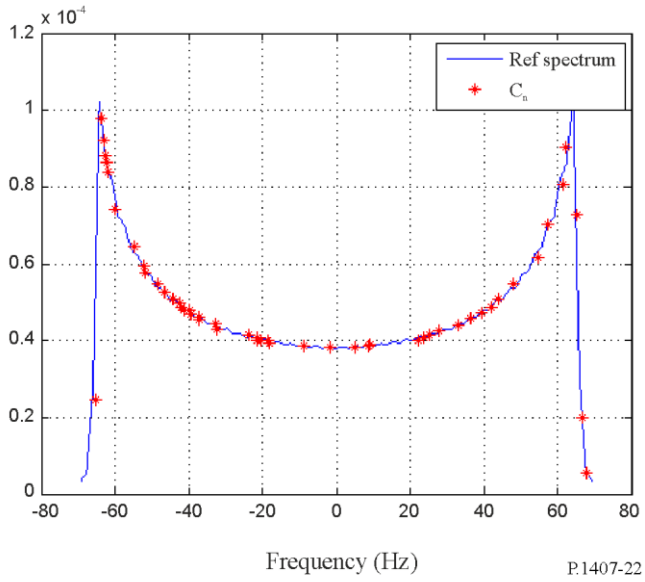

The parameters of the SoS method must be updated during the time series generation i.e. f_n^{Re}, f_n^{Im} should change, and c_n^{Re}, c_n^{Im} as recommended in the two-step procedure. During one-time series generation, it is recommended to change at least 200 times to well reproduce the Doppler spectrum shape. Example is shown in Fig. 23.

FIGURE 23

Earth space spectrum (from Recommendation ITU-R P.681) generation example
Environment = suburban, Frequency = 2 GHz, Elevation = 40°

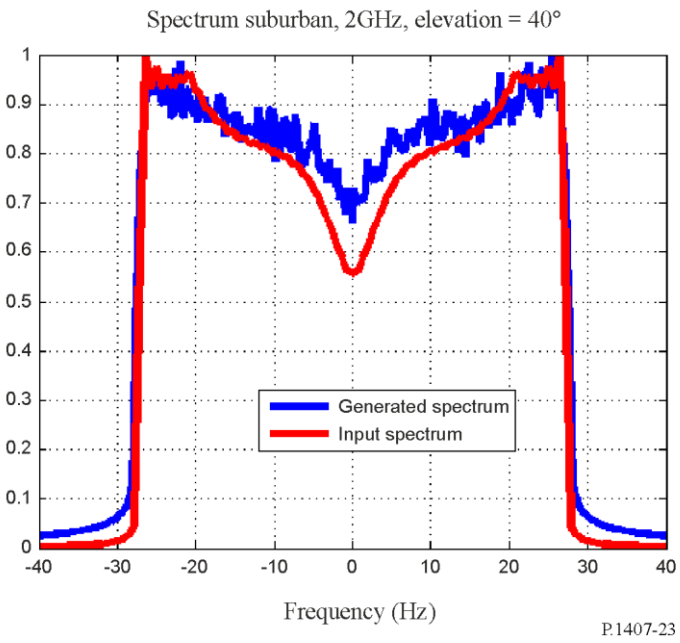

In the very specific case of Jake's Spectrum (as presented in equation (24)), the coefficients of the SoS can be estimated by:

$$c_n^{Re} = c_n^{Im} = \sigma_0 \sqrt{\frac{2}{N}}$$

$$f_n^{Re} = f_n^{Im} = f_{max} \sin\left(\pi \frac{2n-1}{4N}\right)$$

With σ_0 the integral of the Doppler power density, and $f_{max} = \frac{v}{\lambda}$ the maximum Doppler frequency which depends on the wavelength λ and the receiver speed v. In such approach, we recommend to use $N \geq 7$ in order to have a good approximation of the Gaussian process and Doppler power density.

Annex 4

The Rician *K* factor defined as the ratio of the power of the dominant or LoS component to the scattered component, which is defined in Recommendation ITU-R P.1057 as:

$$K = 10 \log\left(\frac{a^2}{2\sigma^2}\right) \quad \text{dB} \tag{39}$$

can be estimated using the method of moments given in equation (40), which can be applied either to (i) a narrowband time variant signal, (ii) a multipath component in a time variant impulse response, or (iii) from the small-scale time variant frequency function of a wideband signal as in Fig. 12 where the Rician *K* value can be estimated from the mean of the K_j values estimated at each frequency, f_j where values when *a* is imaginary are discarded from the estimation of the mean.

$$a = \sqrt[4]{2m_2^2 - m_4} \text{ and } \sigma^2 = \frac{1}{2}(m_2 - a^2) \quad (40)$$

where m_2 and m_4 are the second and fourth order moments as estimated from the data probability density function, $f(x)$, as given by :

$$m_n = \int_{-\infty}^{\infty} x^n f(x) dx$$

When $K_j = 0$, the resulting distribution is Rayleigh, and when a is imaginary, the fading of the multipath component does not follow a Rician distribution.